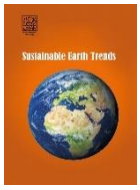
Shahid Beheshti University

Sustainable Earth Trends

Journal homepage: http://sustainearth.sbu.ac.ir



Identifying damage in 3d skeletal structures using a two-stage probabilistic approach by the MTLBO optimization algorithm

Sina Dehyadegari[a*], Ali Keyhani[a]

[a] Faculty of Civil Engineering, Shahrood University of Technology, Shahrood, Iran

ABSTRACT

This paper introduces an advanced structural health monitoring (SHM) framework that integrates Bayesian data fusion with a Modified Teaching–Learning-Based Optimization (MTLBO) algorithm to improve damage identification in space frames and truss structures. The proposed method utilizes multiple vibration-based damage indices, including Modal Strain Energy (MSE), Frequency Response Function Strain Energy (FRFSE), Flexibility Strain Energy (FSE), and Residual Force-Based (RFB) indicators, derived from natural frequencies and mode shapes. These indices collectively enhance damage localization accuracy while reducing the number of false or redundant damaged elements, thereby improving computational efficiency. Through the application of Bayesian data fusion, the approach establishes a robust probabilistic framework that effectively integrates different damage indicators to refine detection results. The incorporation of the MTLBO algorithm further enhances the convergence speed and accuracy of the optimization process, expediting the identification of damage across complex structural systems. Moreover, by employing a probabilistic objective function, the framework demonstrates notable resilience to measurement noise, ensuring reliable performance under uncertain conditions. A key innovation of this study lies in the simultaneous probabilistic treatment of both damage localization and damage severity estimation, enabling more precise, noise-resistant, and computationally efficient damage detection. This hybrid methodology represents a significant advancement in SHM, offering a robust and practical solution for real-world structural assessment and maintenance applications.

ARTICLE INFO

Keywords:
Bayesian fusion
Damage detection
Modify teaching learning-based
Multi-damage detection
Structural health monitoring

Article history:
Received: 26 August 2025
Accepted: 23 October 2025

*Corresponding author
E-mail address:
malekis@scu.ac.ir
(S. Dehyadegari)

Citation:
Dehyadegari, S. & Keyhani, A. (2026). Identifying damage in 3d skeletal structures using a two-stage probabilistic approach by the MTLBO optimization algorithm, *Sustainable Earth Trends:* 6(4), (42-64).

DOI: 10.48308/set.2025.241268.1153

1. Introduction

Structural damages resulting from overloading, corrosion, seismic activity, or material degradation pose a significant threat to human safety and the environment. Structural Damage Identification (SDI), as a preventive tool, enables the assessment of structural health and mitigates potential environmental consequences (Tibaduiza Burgos et al., 2020). Structural failures can lead to both direct and indirect environmental impacts, including contamination of natural resources, such as the leakage of chemicals and pollutants into soil and water; generation of construction waste, as seen in the collapse of buildings and industrial structures; destruction of habitats and ecosystems; and airborne and acoustic effects, including the release of particulate matter and high-intensity noise (Shekhar et al., 2023). Timely identification of structural damage enables repair and reinforcement before catastrophic failures occur, thereby preventing both economic and environmental consequences. So, detecting structural damage is critical across several fields, including civil engineering, mechanical engineering, and aerospace. Among the numerous methods developed, vibration-based techniques have gained significant attention due to their non-destructive nature, cost-effectiveness, and operational convenience methods rely on damage-induced alterations in

Copyright: © 2026 by the authors. Submitted for possible open access publication under the terms and conditions of the Creative Commons Attribution (CC BY). license (https://creativecommons.org/licenses/by/4.0/).

structural modal parameters, such as natural frequencies, mode shapes, and damping ratios (Cruz and Salgado, 2009; Vamvoudakis-Stefanou et al., 2018). While mode share measurements across multiple points render them time-intensive and complex, and damping ratios are challenging to measure due to sensitivity to environmental factors like humidity and temperature, natural frequencies offer a simpltive (Salawu, 1997; Montalvao et al., 2006). Natural frequencies can be measured accurately and reliably with a single sensor placed at any accessible point on the structure (with exceptions for nodes of particular modes (Zhang et al., 2013; Alkayem and Cao, 2018). Consequently, frequency-based damage detection was adopted. Past research highlights various approaches to utilizing modal parameters for damage detection. Pandey and Biswas, for instance, leveraged flexibility matrices to identify structural damage (Radzieński et al., 2011), while Shi and Law introduced the strain energy ratio technique pointing damage locations (Pandey and Biswas, 1994). Additionally, Yan et al. applied Principal Component Analysis (PCA) to detect alterations in vibration characteristics due to environmental effects or structural degradation, proving effective for both linear and nonlinear structures through numerical and experimental studies. Spectral techniques have also been widely used for damage quantification in nonlinear systems (Shi et al., 2002; Yan et al., 2005). This growing body of research underscores the potential of vibration-based tools for structural health monitoring, helping to preemptively identify damage and prevent catastrophic failures. Over the years, researchers have employed a range of vibration-based parameters such as natural frequencies, damping ratios, frequency response functions, modal strain energy, modal residual forces, spectral strain energy, and mode shape curvature for detecting damage across diverse structures, including isotropic trusses, beams, plates, bridges, and composite laminates. In addition, several studies have investigated combining multiple damage indicators, such as pairing natural frequency with mode shapes or combining mode shapes with static displacement, to enhance detection accuracy in various structural types. Each damage parameter offers unique advantages and faces specific limitations, underscoring the importance of selecting the most suitable parameters for effective vibration-based damage detection approach highlights the potential for hybrid methods that leverage multiple indicators to achieve a more robust damage detection process tailored to the demands of particular structural applications (Vamvoudakis-Stefanou et al., 2018). Kim and Stubbs proposed a damage index utilizing modal parameters specifically designed to detect damage in continuous beams. Their method provides a valuable tool for identifying structural damage by analyzing shifts in modal characteristics, contributing to the broader field of vibration-based damage detection methodologies (Machado et al., 2017). Humar et al. performed a comparative analysis of various damage indices derived from frequency, mode shapes, flexibility, and modal residual force, evaluating their effectiveness in accurately identifying structural damage (Kim and Stubbs, 2002). Their study provided critical insights into the relative strengths of each index for specific applications in damage detection. Similarly, Shih et al. developed a damage detection algorithm for plate structures that integrates modal flexibility, modal strain energy, and natural frequency (Humar et al., 2006).

Mario D. et al. develops a vibration-based finite element method to predict damage in composite concrete–steel beams. A quasi-static four-point bending test is simulated, and the model equations are modified via the Newton–Raphson method to account for stiffness degradation. Modal analysis of the stressed state captures changes in natural frequencies and modal shapes, forming a damage index. The approach effectively predicts damage during construction, service, or accidental loads, enhancing structural safety and advancing vibration-based damage detection for composite systems (Cedeño-Rodríguez et al., 2025).

This multi-parameter approach aims to enhance detection accuracy and minimize the risk of false positives, highlighting the importance of leveraging multiple indices to improve reliability in structural health monitoring. Fan and Qiao conducted a review of literature and recommended mode shape curvature-based algorithms as more reliable for damage detection compared to frequency and mode shape-based algorithms (Fan and Qiao, 2011). Additionally, Das et al. performed a comparative study on various dynamic

parameters, revealing that timeseries data exhibit higher sensitivity to damages than frequency domain parameters (Shih et al., 2009). Cao et al. highlighted damping as a highly effective damage indicator, particularly when combined with frequency or mode shapes, provided that suitable damping measurement techniques are employed (Das et al., 2016). When discussing vibration-based damage detection, the focus naturally shifts towards optimization-based inverse techniques. Various optimization algorithms have been employed by researchers to address the challenges posed by inverse damage detection. These algorithms encompass genetic algorithm, artificial neural network (ANN), ant colony optimization (ACO), immunity enhanced particle swarm optimization (IEPSO), particle swarm optimization (PSO), antlion optimization (ALO), unified particle swarm optimization (UPSO), dynamic hybrid adaptive firefly algorithm (DHAFA), teaching learning-based optimization (TLBO), artificial bee colony (ABC), aging leader challenger particle swarm optimization (ALC-PSO), and enhanced PSO with intelligent particle number (IPNPSO). The convergence speed, ability to navigate local minima, and result accuracy are among the key distinguishing factors of these optimization algorithms. Most of these computational methodologies demonstrate satisfactory efficacy in the detection of damage within small-scale structures. However, only a limited number of these approaches have proven to be effective when applied to larger structures, where the search space for potential damage locations significantly increases due to the structure's size. The probability of attaining the global optimum within a specific number of iterations decreases as the problem's magnitude grows. Therefore, the selection of suitable optimization algorithms is paramount for obtaining precise results in inverse damage identification scenarios. It should be emphasized that each optimization algorithm has its own restrictions regarding the range of search space it can efficiently handle. Furthermore, the computational time rises substantially with the enlargement of the search space, as larger-scale problems demand a bigger population size for optimization purposes. Consequently, the main challenges linked to conventional optimization-based single-stage damage detection methods revolve around limitations associated with the size of the search space and the slow rate of convergence when addressing larger issues (Mishra et al., 2020). In the latest research explores 1D CNNs for damage detection across populations of structural components. A CNN is trained on simulated vibration data from aluminum beams with randomly modeled damage and validated on experimental data. Particle Swarm Optimization fine-tunes convolutional kernels for optimal feature extraction. The method achieves near-perfect accuracy on simulated data and distinguishes damaged from undamaged beams in experiments with 76.3% accuracy, outperforming traditional ML approaches. This demonstrates the potential of 1D CNNs to detect damage across multiple structures using a single model (Ruiz et al., 2025).

In another study, a method for beam damage detection based on Frequency Response Functions (FRFs) is presented. Experimental data were collected from five aluminum beams, both healthy and damaged, with rectangular notches introduced to simulate damage. A stochastic finite element model in MATLAB was employed to generate training data, and damage was simulated by reducing the cross-sectional area of the elements. Simple damage indices were introduced as damage-sensitive features, and three classifiers—Decision Tree, SVM, and Artificial Neural Network—were trained for damage detection and localization. The neural network demonstrated the best performance, achieving 99.3% accuracy in detection and 80–97% accuracy in localization during the training phase. Although accuracy decreased during validation, the method remained effective in regions distant from the excitation points (Ruiz et al., 2024).

Two-stage methods, conversely, rely on the utilization of damage indices in the initial phase, succeeded by the implementation of optimization procedures in the subsequent phase, which possess the potential to effectively mitigate the limitations associated with single-stage methods as evidenced by various studies (Kaveh and Zolghadr, 2017; Ghasemi et al., 2018). Dinh-Cong et al. implemented a two-stage model reduction technique for the purpose of pinpointing damage locations within trusses (Dinh-Cong et al., 2019). Moreover, three-stage methodologies for damage detection are also prevalent in the realm of structural engineering (Gerist and Maheri, 2016). Nevertheless, these

methods are not devoid of limitations. Frequently, information pertaining to damage extracted from a singular damage index may lack reliability, potentially leading to the identification of additional damaged elements alongside the actual damaged components. Furthermore, the value of a particular element's damage index may exhibit substantial discrepancies across different damage indices when addressing the same damage scenario. Hence, it is strongly recommended to integrate damage information derived from multiple indices prior to drawing conclusions regarding the plausible damage scenario. The fusion of data from diverse sources serves to diminish uncertainties in estimating the requisite parameters and augments the insights garnered from each individual data source as highlighted (Mishra et al., 2019). In another study conducted by Swarup K. Barmanand colleagues, damage identification was performed in two stages using the TLBO algorithm. In this research, a combination of damage indices was utilized solely in the first stage with the help of Bayesian theory. However, the application of Bayesian theory in the second stage and the investigation of a probabilistic objective function using the MTLBO algorithm were not undertaken (Barman et al., 2021).

In an interesting study a two-stage structural damage detection (SDD) method using 2D convolutional neural networks (2D-CNN) on time-domain vibration signals. The method is applied to steel beams and frame-type structures, achieving over 90% accuracy in locating and quantifying single- and multi-damage scenarios from simulated noisy data. Experimental validation with steel frame joints from the Qatar University Grandstand simulator showed 100% accuracy within 10 epochs, outperforming other deep learning algorithms. The main contribution is an effective AI-based approach for multiclass damage identification and quantification in civil structures (Das and Guchhait, 2024).

This study employs a two-phase method designed to reduce computational costs in structures with high degrees of freedom. Initially, a damage identification phase uses a failure index in conjunction with a Bayesian probabilistic approach to locate potential damage with efficiency. Following this, an optimization phase seeks to enhance the precision of damage rate identification by applying the meta-heuristic Modified Teaching-Learning-Based Optimization (MTLBO) algorithm, which has been optimized through prior research (Li et al., 2020). A detailed investigation and comparative analysis of this approach underscore its effectiveness. Additionally, given the impact of noise in practical applications, the integration of a probabilistic objective function becomes essential, substantially minimizing the typical margin of error in the damage detection process. This dual-phase approach highlights the balance between computational efficiency and detection accuracy, offering a robust framework for real-world structural health monitoring. This research investigates the reduction of computational cost through the implementation of a two-step process and the use of a probabilistic objective function to minimize susceptibility to environmental noise. In this approach, damage detection is performed probabilistically in both stages. In the first stage, a probabilistic approach is used to identify members suspected of damage and to reduce the inputs for the second stage. In the second stage, the proposed objective function is employed to reduce the impact of noise. However, the use of this optimization algorithm and the introduced objective function has not been specifically addressed in the studies reviewed. In other words, the use of a probabilistic approach in both stages of the damage detection process is considered a key highlight of this research.

2. Material and methods

2.1. Structural damage identification

This section provides an in-depth discussion on four distinct damage indices based on vibration analysis, highlighting the critical role that careful selection of these indices plays in the success of a two-stage damage detection methodology. The choice of an appropriate damage index depends heavily on the specific structural characteristics of the system under analysis, emphasizing the importance of tailored selection for accurate assessment. Vibration-based damage indices leverage various parameters such as natural frequencies, mode shapes, mode shape curvature, modal flexibility, and modal residual force to enable a holistic evaluation of structural health. Each

damage index possesses a unique range of applicability: some are tailored to continuous systems, while others are optimized for discrete systems. For example, Barman et al. demonstrated the effectiveness of a mode shape curvature-based damage index for detecting damage in composite beams and plates, where the index is calculated at each structural node. However, this curvature-based index is unsuitable for discrete systems, such as trusses and frames, due to their segmented structural configuration. In this study, four versatile damage indices, Damage index based on modal strain energy (DIMSE), Frequency response function strain energy dissipation ratio (FRFSEDR), Flexibility strain energy-based damage ratio (FSEDR), and Residual force-based damage index (RFBDI)have been identified. These indices are applicable across both discrete and continuous systems, broadening their practical utility in structural health assessment and enhancing the adaptability of vibration-based methodologies (Barman et al., 2018; Dinh-Cong et al., 2019).

2.1.1. Damage index based on modal strain energy

Using a damage index based on modal strain energy offers significant insights into both the location and extent of structural damage. This approach begins with the dynamic equation of motion for a vibrating structure under external forces, expressed as Eq. 1:

$$M\ddot{x}(t) + C\dot{x}(t) + Kx(t) = F(t) \quad (1)$$

Where M is the mass matrix, C is the damping matrix, K is the stiffness matrix, u(t) represents the displacement vector as a function of time and F(t) is the external force vector. By analyzing variations in the modal strain energy derived from these parameters, we can evaluate structural health with regard to both potential damage locations and severity, using shifts in vibration characteristics to indicate compromised areas. In structural systems, damage is typically assumed to affect only the stiffness properties while leaving the mass properties unchanged. For a system exhibiting low damping, the eigenfrequencies and mode shapes can be obtained by simplifying the dynamic equation of motion presented earlier. This simplification leads to the following Eq. 2:

$$[K - \lambda_i M]\phi_i = 0 \quad Or \quad [K - \omega_i^2 M]\phi_i = 0 \quad (2)$$

The MSE of intact and damaged structure, respectively, of jth element in ith mode can be defined as Eqs. 3 and 4:

$$MSE_{ij}^{u} = (\phi_i^u)^T K_j^e (\phi_i^u) \quad (3)$$

$$MSE_{ij}^{d} = (\phi_i^d)^T K_j^e (\phi_i^d) \quad (4)$$

ω_i is *i*th eigenfrequency vector and φ_i is *i*th mode shapes vector.

K_i^e is the stiffness matrix of the *j*th element of the undamaged structures.

Solving this eigenvalue problem allows us to extract the eigenfrequencies(ω)and the corresponding mode shapes, which are essential for assessing the structural integrity and identifying potential damage locations based on changes in these parameters. This relationship highlights the sensitivity of the system's dynamic response to alterations in stiffness due to damage. Now, damage index for *j*th element can be calculated as Eq. 5:

$$D_{1j} = \frac{\sum_{i=1}^{m} \gamma_{ij}^{d}}{\sum_{i=1}^{m} \gamma_{ij}^{u}} - 1 \quad (5)$$

m is number of modes considered.

γ_{ij}^{u} and γ_{ij}^{d} can be obtained as Eqs 6, 7, and 8:

$$\gamma_{ij}^{u} = \frac{MSE_{ij}^{u}}{\sum_{j=1}^{n_{ele}} MSE_{ij}^{u}} \quad (6)$$

$$\gamma_{ij}^{d} = \frac{MSE_{ij}^{d}}{\sum_{j=1}^{n_{ele}} MSE_{ij}^{d}} \quad (7)$$

$$U_1 = \frac{D_1}{\sum_{j=1}^{n_{ele}} D_{1j}} \quad (8)$$

The vector representing the extent of damage can be denoted as $D_1 = \{D_{11}, D_{12}, ..., D_{1nele}\}'$.

When developing damage indicators for structures, it is postulated that the damage

indicator will exhibit a non-negative value or zero, where zero signifies undamaged elements and a positive value indicates the presence of damage. The negative values of the damage index do not hold any physical significance. Previous studies by researchers have adhered to similar assumptions in formulating damage indicators for structures using Modal Strain Energy (MSE) (Humar et al., 2006; Ghiasi et al., 2019). This study also adopts a similar assumption. The damage index values DIMSE obtained are then transformed into probability values U_1 for the purpose of applying Bayesian fusion technique, achieved by normalizing within the range [0,1] based on the 8equation.

2.1.2. Frequency response function strain energy dissipation ratio (FRFSEDR)

A strain energy-based index for the Frequency Response Function has been introduced, with a modified damage index termed FRFSEDR derived using a similar methodology (Bagherahmadi and Seyedpoor, 2018). In this approach, the formulations for external harmonic forces and the corresponding responses in the dynamic Eq. 1 can be expressed accordingly (Eqs. 9 and 10).

$$F(t) = F(\Omega)e^{-p\Omega t} \tag{9}$$

$$x(t) = x(\Omega)e^{-p\Omega t} \tag{10}$$

By placing (Eq. 9) and (Eq. 10) in Eq. 1, we get the following Eq. 11. Here, the function H(Ω) can be derived in accordance with Eq. 12.

$$x(\Omega) = H(\Omega)F(\Omega) \tag{11}$$

$$H(\Omega) = \phi \text{diag}\left(\frac{1}{\omega_i^2 - 2\Omega p\omega_i\zeta_i - \Omega^2}\right)\phi^T \tag{12}$$

ω_i is circular frequency and ζ_i is modal damping ratio of the structure for *ith* mode.

A damage index is now formulated by utilizing the alteration in strain energy of both damaged and intact structures, which is derived from the FRF matrix H. Initially, circular frequencies and mode shapes for both undamaged and damaged structures were computed as outlined in Eq. 2. Subsequently, the FRF matrix for undamaged and damaged structures can be derived from Eq. 12. In practical scenarios, the FRF matrix would manifest as a three-dimensional matrix owing to the presence of excitation frequency. Nevertheless, for the current scenario, the excitation frequency Ω is assumed to be zero, leading to the conversion of the FRF matrix into a two-dimensional flexibility matrix. Consequently, the frequency response change matrix (FCM) can be computed as follows (Eq. 13):

$$F_{CM} = FRF^u - FRF^d \tag{13}$$

Each column within the Finite Element Compliance Matrix (FCM) illustrates the alteration in nodal displacement configuration resulting from the application of a unit harmonic force on the specific degree of freedom associated with that column. Consequently, the variation in the accumulated elastic potential energy, known as the Formulation Strain Energy (FSE), within the *i*th column of the *j*th element can be determined by utilizing the FCM in the following manner (Eq. 14):

$$FSE_{ij} = (F_{CM})_i^T K_j^e (F_{CM})_i \tag{14}$$

The damage index (D) for the j-th element can now be computed in the following manner (Eq. 15).

$$D_{2j} = \frac{\sum_{i=1}^{n_{col}} \left(\frac{FSE_{ij}}{\max_i\left(FSE_{ij}\right)}\right)}{n_{col}} \tag{15}$$

n_{col} is the number of columns in *FCM* matrix.

the damage index vector can be expressed as $D_2 = \{D_{21}, D_{22}, ..., D_{2nele}\}'$.

The damage index values FRFSEDR acquired have been transformed into probability values U_2 to facilitate the application of the Bayesian fusion technique by normalization within the interval [0,1] using the specified Eq. 16.

$$U_2 = \frac{D_2}{\sum_{j=1}^{n_{ele}} D_{2j}} \quad (16)$$

2.1.3. Flexibility strain energy-based damage ratio (FSEDR)

A novel strain energy-based damage index called FSEDR, which is rooted in modal flexibility, has been formulated for the purpose of identifying structural damages. The flexibility matrix (S) is defined as the reciprocal of the stiffness matrix K, and its computation can be derived from the dynamic responses acquired through modal analysis, as elucidated in Eq. 17 (Ghiasi et al., 2019).

$$F = [\phi][\Lambda]^{-1}[\phi]^T \simeq \sum_{i=1}^{m} \frac{1}{\omega_i^2}\phi_i\phi_i^T \qquad [\Lambda] = diag(\frac{1}{\omega_i{}^2}) \quad (17)$$

m is the number of considered modes.
Flexibility matrices for both the sound structure (S_u) and the impaired structure (S_d) have been computed based on the responses of undamaged and damaged structures, respectively. Subsequently, a specific column within a flexibility matrix can be denoted as the pattern of displacement for all degrees of freedom when a unit load is exerted on the corresponding degrees of freedom, meaning that the ith column of the flexibility matrix illustrates the displacement pattern exhibited by the structures under a unit load on the ith degrees of freedom. Consequently, the computation of strain energy can be achieved by utilizing each column of the flexibility matrix. Therefore, the total strain energy of the j-th element for ncol columns of the flexibility matrix can be determined as Eqs. 18 and 19:

$$FSE_{ij}^u = (s_i^u)^T K_j^e (s_i^u) \quad (18)$$

$$FSE_{ij}^d = \left(s_i^d\right)^T K_j^e \left(s_i^d\right) \quad (19)$$

S_i is the ith column of the flexibility matrix.
n_i is number of columns in flexibility matrix.
Damage index of j^{th} element can be calculated as Eq. 20:

$$D_{3j} = \frac{\sum_{i=1}^{n_{col}} v_{ij}^d}{\sum_{i=1}^{n_{col}} v_{ij}^u} - 1$$

$$v_{ij}^u = \frac{FSE_{ij}^u}{\sum_{j=1}^{n_{ele}} FSE_{ij}^u} \quad (20)$$

$$v_{ij}^d = \frac{FSE_{ij}^d}{\sum_{j=1}^{n_{ele}} FSE_{ij}^d}$$

The vector representing the extent of damage can be denoted as $D_3 = \{D_{31}, D_{32}, ..., D_{3nele}\}'$. The same assumption as detailed in Section 2.1 has been taken into account in order to derive the ultimate values of D_3. Consequently, a damage index value of 0 is assigned to the undamaged element, while a value greater than 0 is assigned to the damaged element. The obtained damage index values FSEDR have been transformed into probability values U_3 to facilitate the application of Bayesian fusion technique by normalizing them within the interval [0,1] using the provided Eq. 21 (Niu et al., 2019).

$$U_3 = \frac{D_3}{\sum_{j=1}^{n_{ele}} D_{3j}} \quad (21)$$

2.2. Residual force-based damage index (RFBDI)

Modal residual force can be utilized in the identification of structural damages. The eigenvalue equation for a damaged structure can be formulated by modifying Eq. 2 as presented in Eq. 22.

$$(K + \delta K)\phi_i^d - \lambda_i^d M\phi_i^d = 0 \quad (22)$$

λ_i^d represents the itheigenvalue of damaged structures.
δK denotes the alteration in the damage matrix caused by the presence of damage.
The Eq. 22 can be expressed in the subsequent form Eq. 23:

$$K\phi_i^d - \lambda_i^d M\phi_i^d = R_i = -\delta K\phi_i^d \quad (23)$$

R_i is defined as the modal residual vector for the i^{th} mode and can be computed by evaluating the left-hand side of (Eq. 23). The parameter δK can be represented in the form Eq. 24:

$$\delta K = -\sum_{j=1}^{n_{ele}} \eta_j K_j^e \quad (24)$$

K_j^e signifies the element stiffness matrix of the j^{th} element and η_j indicates the stiffness variation in element j. By combining the right-hand side of Eqs 23 and 24 for the i^{th} mode, we obtain Eqs. 25 and 26:

$$\left(\sum_{j=1}^{n_{ele}} \eta_j K_j^e\right) \phi_i^d = R_i \quad (25)$$

, or as

$$A_i \beta_i = R_i \quad (26)$$

A_i stands for an unsymmetrical matrix for the i^{th} mode. β_i represents a vector that specifies elemental stiffness changes for the i^{th} mode and is denoted by $\beta_i = \{\eta_1 . \eta_2 . \ldots \eta_{n_{ele}}\}_i'$ (Eq. 27).

$$\beta_i = A_i^+ R_i \quad (27)$$

A_i^+ corresponds to the Moore-Penrose generalized inverse matrix of A_i. Each element of β_i falls within the interval [0,1] where 0 denotes no damage, while 1 indicates complete damage. The vector β_i can be generated for every mode. Subsequently, β_i is normalized by dividing each of its components by the sum of all β_i values in each mode. Eventually, the normalized vectors are averaged across m modes to compute the elemental damage index vector D_4 as Eq. 28:

$$D_4 = \frac{\sum_{i=1}^{m} (\beta_i)}{m} \quad (28)$$

D_4 vector has dimensions $[n_{ele} \times 1]$. The RFBDI value for each element can be determined as follows (Eq. 29):

$$D_{4j} = D_4(j, 1) \quad (29)$$

The obtained damage index values RFBDI are converted into probability values U_4 to facilitate the application of the Bayesian fusion technique by normalization within the range [0,1] utilizing the following equation.

2.3. Bayesian data fusion

The Bayesian approach has established itself as a robust methodology in the field of damage detection through vibration measurements, boasting a rich history of application. Its strengths are particularly evident in the area of uncertainty quantification within model updating processes, where it provides a comprehensive understanding of uncertain parameters and their complex interactions. This approach facilitates the integration of diverse data sources, encompassing numerical experiments, laboratory testing, and real-world structural observations. By synthesizing information from these varied sources, the Bayesian methodology enhances the reliability and accuracy of damage detection assessments. It enables the quantification of uncertainty in model parameters, allowing for more informed decision-making and effective risk management in structural health monitoring. The versatility of this approach makes it applicable across a wide range of scenarios, underscoring its significance in advancing the field of structural engineering and safety (Simoen et al., 2015). Numerous researchers have leveraged the oscillation-based Bayesian methodology for detecting structural impairments across a wide variety of constructions. These scholars have utilized a range of vibration parameters and responses, such as natural frequencies and mode shapes, to identify damages effectively. In addition to these traditional metrics, incomplete retort information and time-domain data have also been applied in this context, enhancing the robustness of the damage detection process. Modal strain energy has emerged as another valuable parameter for assessing structural integrity. Furthermore, the integration of Central Difference Filter (CDF) within the framework of Recursive Bayesian Filtering (RBF) has been explored by Chen and Feng.

Their work aims to develop a continuous health monitoring algorithm for structures, demonstrating the potential of advanced filtering techniques to enhance the accuracy and efficiency of real-time structural assessments. This comprehensive approach underscores the versatility and efficacy of Bayesian methodologies in advancing structural health monitoring practices (Simoen et al., 2015). Similarly, Prakash and Narasimhan have suggested a Bayesian two-stage gamma process model aimed at boosting damage detection capabilities by discriminating between progressive damage arising from aging or operational circumstances, and abrupt damage originating from shocks or impacts (Montazer and Seyedpoor, 2014). The flexibility of the Bayesian methodology is further emphasized by its successful application in identifying impairments across various practical structures such as bridges, railway ballasts, masonry heritage structures, steel bolted connections, plate structures, trusses, and steel frames. In the current investigation the diverse impairment indicators documented in Section 2.1 are amalgamated at single phase by Bayesian information amalgamation. The impairment index arrays $(D_1, D_2, D_3 \; and \; D_4)$ are transformed to likelihood values $U_1, U_2, U_3 \; and \; U_4$ before data amalgamation as referenced in preceding sections. The impairment preceding likelihood is presupposed to be equivalent before implementing the various impairment indicators, i.e. $P(X) = 1/n_{ele} \; with \; \sum_{j=1}^{n_{ele}} P(x_j) = 1$, here n_{ele} is the quantity of elements discretized in the pattern for potential impairment. For pattern with m quantity of impairment indicators (Y_1, Y_2, ..., Y_m), each impairment indicator providing an additional acquaintance about likely impairment locations, the formulation for Bayesian information amalgamation utilized is provided as Eq. 30:

$$P(X_i \mid Y_1, Y_2, \ldots, Y_m) = \frac{\prod_{k=1}^{m} P(Y_k \mid X_i) P(X_i)}{\sum_{j=1}^{n_{ele}} \prod_{k=1}^{m} P(Y_k \mid X_j) P(X_j)} \tag{30}$$

Here, U_{1i}, U_{2i}, U_{3i}, U_{4i} are the likelihood values acquired from the column matrices $U_1, U_2, U_3 \; and \; U_4$ respectively corresponding to ith element. Bearing these details in consideration, the current investigation concentrates on constructing a durable impairment identification methodology grounded on vibration parameters such as frequencies, mode shapes, and modal flexibility utilizing Bayesian information amalgamation methodology. The flowchart for the proposed approach is shown in Fig. 1.

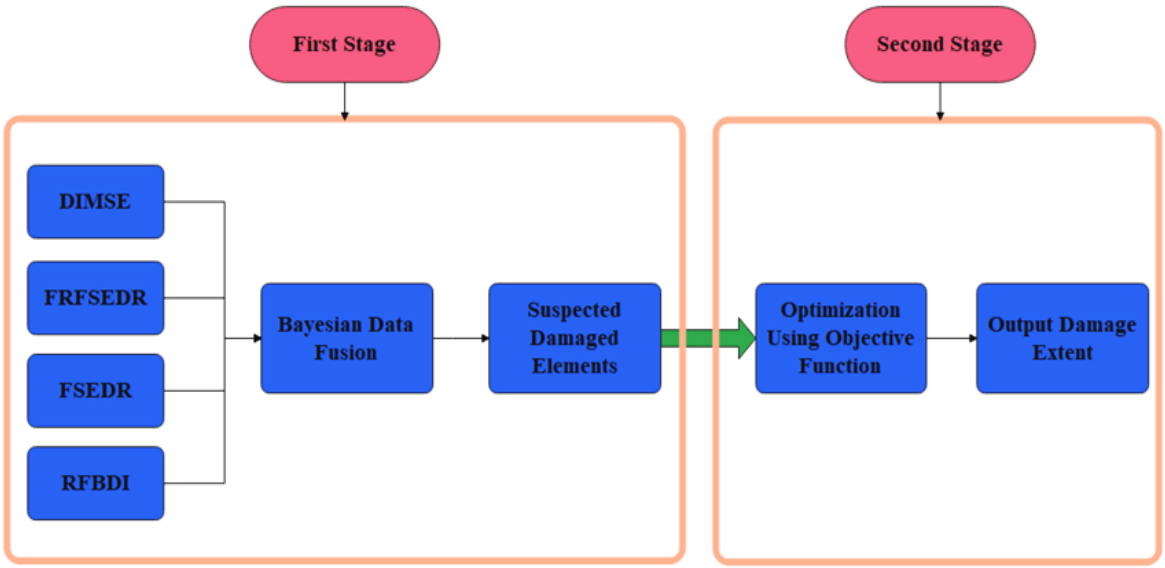


Fig. 1. Flowchart for the proposed approach.

2.4. Optimization algorithm

A modified teaching–learning-based optimization algorithm (MTLBO) are proposed by (Niu et al., 2019), which enhances the original TLBO in several noteworthy manners. One of the principal advantages of MTLBO over TLBO is its capacity to yield superior solution quality and expedited convergence. MTLBO accomplishes this by incorporating more sophisticated learning mechanisms in both the instructor and learner phases. Specifically, MTLBO categorizes the population into two cohorts: exemplary students and underperformers, predicated on their performance relative to the class mean. This differentiation allows exemplary students to acquire knowledge both autonomously and from other high-achieving individuals, while underperformers predominantly gain insight from the instructor. This methodology engenders a more heterogeneous learning process, which aids the algorithm in exploring the search space more efficiently, thereby diminishing the likelihood of becoming ensnared in local optima. Furthermore, the incorporation of inertia weights to regulate the equilibrium between exploration and exploitation further augments the algorithm's capability to identify optimal solutions in a prompt manner. The MTLBO proffers several optimization solutions that render it more effective than TLBO. One of the principal innovations is the introduction of the "Actual Teaching-Learning Situation" (ATLS), which emulates real-world classroom dynamics. In MTLBO's instructor phase, exemplary students, who achieve scores above the mean, benefit from both independent study and interactions with the highest-performing student, whereas underperformers predominantly depend on their instructor for knowledge. This differentiation ensures that students (or candidate solutions) with superior performance are utilized to enhance the overall solution quality, while weaker individuals receive targeted guidance to elevate their performance. Moreover, in the learner phase, students are also stratified into exemplary and underperformer groups, with exemplary students not only interacting with peers but also engaging in independent study, while underperformers continue to rely on the instructor. This mechanism enables MTLBO to sustain diversity and avert premature convergence (Mishra et al., 2019).

2.5. Teacher phase

In this phase, all students are divided into two groups based on the mean value of the class room. One group contains the superior students, another includes the underachievers. We assume that if one student's comprehensive mark is higher than the mean mark of the class, the student is considered as a superior student. Otherwise, the student is regarded as an underachiever. In this paper, the proposed MTLBO is used to solve the minimum optimization problem, so the individual presents the best performance with the lowest fitness value. In MTLBO, for a superior student, he can get knowledge from the best individual and study independently. The meaning of study independent is that the superior student still searches the optimal solution along with his previous information direction. For an underachiever, he obtains knowledge from his teacher. Based on the above analysis, the solution updating mechanism is shown in Eq. 31. Moreover, the expression of inertia weight is presented in Eq. 32. The $X_{new}$is accepted if it gives a better function value.

$$X_{\text{new},i} = \begin{cases} X_{\text{old},i} \times \omega + \left(X_{\text{best}} - X_{\text{old},i}\right) \times \text{ rand} & \text{if } f\left(X_{\text{old},i}\right) \le f\left(X_{\text{mean}}\right) \\ \left(X_{\text{old},i} + (\text{ rand } - 0.5) \times 2 \times \left(X_{\text{mean}} - X_{\text{old},i}\right)\right) \times \sin\left(\frac{\pi}{2} \times \frac{\text{iter}}{\text{MaxIter}}\right) + \cdots & \\ \text{diff} \times \cos\left(\frac{\pi}{2} \times \frac{\text{iter}}{\text{MaxIter}}\right) & \text{if } \quad f\left(X_{\text{old},i}\right) > f\left(X_{\text{mean}}\right) \end{cases} \tag{31}$$

$$W = \omega_{\text{start}} - \left(\omega_{\text{start}} - \omega_{\text{end}}\right) \times \frac{\text{iter}}{\text{MaxIter}} \tag{32}$$

Seen from Eq. 31, X_{mean} is the mean result, W is the inertia weight which decides to balance the exploration and exploitation ability. Additionally, we also introduce $\sin(\frac{\pi}{2} \times \frac{iter}{MaxIter})$ and $\cos(\frac{\pi}{2} \times \frac{iter}{MaxIter})$ as inertia weights which can accelerate the convergence speed. *iter* is the current iteration, *MaxIter* is the maximum iteration. Seen from Eq. 32, the inertia weight

descends linearly from ω_{start} to ω_{end}. Therefore, the adjustment process of inertia weight allows the MTLBO algorithm to explore the search space in the initial steps and to exploit the optimal solution in the latter steps. So, the teacher plays an important role to improve the student's knowledge in the initial step. With the running of MTLBO, all individuals close to the optimal solution gradually if the algorithm shows good global convergence ability. Therefore, to avoid trapping into local optimum, the diversity of the population is increased in the latter step. Based on the analysis, the solution quality and convergence speed of MTLBO are indeed enhanced by the two inertia weights.

2.6. Learner phase

After teacher phase, the fitness values of all learners are sorted in ascending order. Then, the students are divided into two groups, where the first group includes the top half students and the second group contains the remaining students. The first group members are regarded as superior students, so they can not only obtain knowledge from a more superior student, but also study independently. The second group members get knowledge from their teacher principally. Therefore, the first group students update their results based on Eq. 33. On the contrary, the second group learners update their results according to Eq. 34 (Mishra et al., 2019).

$$\begin{aligned}&\text{if } f\left(X_{\text{old},i}\right) > f\left(X_{\text{neighbour}}\right)\\&X_{\text{new},i} = X_{\text{old},i} + \left(X_{\text{neighbour}} - X_{\text{old},i}\right) \times \cos\left(\frac{\pi}{2} \times \frac{\text{iter}}{\text{Maxter}}\right)\\&\text{else}\\&X_{\text{new},i} = X_{\text{old},i} + (\text{ rand } - 0.5) \times 2 \times \left(X_{\text{upper limit}} - X_{\text{lower limit}}\right)\\&\text{end}\end{aligned} \tag{33}$$

$$X_{\text{new},i} = X_{\text{old},i} + \left(X_{\text{best}} - X_{\text{old},i}\right) \times \cos\left(\frac{\pi}{2} \times \frac{\text{iter}}{\text{MaxIter}}\right) \tag{34}$$

Shown in Eq. 33, in *j*th iteration, for a learner X_i, randomly selects a learner $X_{neighbour}$, where *neighbour*≠i. If $X_{neighbour}$ has a smaller fitness value than X_i, the student X_i will obtain the knowledge from $X_{neighbour}$; otherwise, he will learn knowledge by himself. Based on this kind of mechanism, the diversity of the population will be increased and the convergence speed will be quickened simultaneously. For the second group members, there is a big gap between the latter of half learners and the teacher, so a big correction is needed to improve the learner's mark. Also, the convergence speed is accelerated obviously (Niu et al., 2019).

2.7. Consideration of noise

Every algorithm must possess the capability to address the uncertainties stemming from measurement errors that are inherent in the experimentally derived responses of actual structures (Mishra et al., 2019). In the current research investigation, intrinsic noise has been integrated with the numerically acquired natural frequencies (f) and mode shapes (φ) to emulate the uncertain conditions prevalent in real-world scenarios. The incorporation of noise within the frequencies and mode shapes is delineated in the present research study (Eqs. 35 and 36):

$$f_{noise} = f_{analitycal}\left(1 + \frac{rand[-1,1] \times \delta}{100}\right) \tag{35}$$

$$\phi_{noise} = \phi_{analitycal}\left(1 + \frac{rand[-1,1] \times \delta}{100}\right) \tag{36}$$

3. Results and discussion

In this particular segment, the efficacy of the meticulously crafted two-stage methodology that integrates Bayesian fusion with a metaheuristic algorithm has been thoroughly illustrated through the use of several exemplars pertaining to the detection of structural damage, which is fundamentally grounded in the analysis of vibration parameters. To facilitate an accurate assessment of any potential damage, the initial six vibrational modes have been systematically employed for each individual structure, thus allowing for a comprehensive evaluation of their integrity. Following this initial analysis, the forthcoming subsections will elucidate the process whereby the first stage, which is predicated on Bayesian fusion principles, is subsequently succeeded by a second stage that is firmly anchored in

metaheuristic strategies, all aimed at the effective identification of damage within the sample structures under consideration.

3.1. Bayesian fusion-based first stage

In this segment, the Bayesian fusion methodology has been meticulously applied to the four previously mentioned damage indices outlined in section 2, with the explicit objective of isolating and identifying the elements within the damaged structures that are suspected to be compromised. In order to enhance the visual representation of the probable damaged elements, the graphical representations of the results obtained through Bayesian fusion have seen the Bayes norm and the actual damage severity being transformed into coded integer values, which serve to facilitate a more intuitive understanding of the data. This transformation was deemed essential due to the significant disparity in the ranges of the values, as the Bayes norm fluctuates between 0.0001 and 0.1, while the actual damage severity spans a broader spectrum, varying from 0.1 to 1. The criteria for establishing these coded values were determined through a systematic approach, ensuring that they accurately reflect the underlying data while also providing clarity and coherence in the representation of the findings.

1. if x ∈ [0, 0.0001], x(coded)] = 0
2. if x ∈ [0.0001, 0.001), x(coded)] = 1
3. if x ∈ [0.001, 0.01), x(coded)] = 2
4. if x ∈ [0.01, 0.1), x(coded)] = 3
5. if x ≥ 0.1, x(coded) = 4

3.2. Metaheuristic algorithm-based second stage

In this section, suspected damage locations obtained from the Bayesian fusion for a threshold limit of 0.0001 have been considered for the second-stage of damage detection. "In the following, to determine the severity of the damage based on the suspected members, the first stage of the MTLBO metaheuristic algorithms is used."

3.2.1. Objective function for present study

To remove the noise negative effect from the optimal process, the idea of Bayesian theory is referred to form a more effective objective function and help to distinguish spurious damaged elements out of the solution. The probabilistic Structural Health Monitoring (SHM) framework grounded in Bayesian theory was introduced and applied in a simulated online monitoring context (Hızal and Aktas, 2021). At the core of Bayesian theory lies conditional probability, which relies on prior knowledge associated with specific events or hypotheses. The Bayesian interpretation provide a rigorous process for uncertainty quantification. Bayesian theory used in the SHM field to express the updated probabilities of model parameter θ has the mathematical form as Eq. 37:

$$p(\theta \mid \mathrm{D}) = cp(\mathrm{D} \mid \theta)p(\theta) \tag{37}$$

where $p(\theta|\mathrm{D})$ is probability density function (PDF) of model parameters given the modal data D and the assumed FEM, and $p(D|\theta)$ is PDF of modal data given the model parameter θ, which is more widely known as likelihood function. $p(\theta)$ is prior PDF of model parameters θ based on engineering and modeling judgments. c is a constant which ensures the integral of $p(\theta|D)$ to be one. Taking D= [D_1, D_2…, D_{Ns}] as observing modal data with N_s samples, D_s= [$\omega_{1,s}$, $\omega_{2,s}$, …,$\omega_{m,s}$, $\varphi_{1,s}$, $\varphi_{2,s}$,…, $\varphi_{m,s}$] represents the s-th sample of frequencies and mode shapes. Then the likelihood function becomes (Eq. 38):

$$p(\mathrm{D} \mid \theta) = \prod_{s=1}^{N_s} p(\mathrm{D}_s \mid \theta) = \prod_{s=1}^{N_s} \left(\prod_{m=1}^{N_m} p(\omega_{m,s}^{ur} \mid \theta) p\left(\varphi_{m,s}{}_{m,s}^{ur} \mid \theta\right) \right) \tag{38}$$

It is assumed that test and modal data are independent. The principle of maximum entropy is used as a justification to choose a Gaussian distribution for $\omega_{m,s}$, and $\varphi_{m,s}$. Then the resulting PDFs of $\omega_{m,s}$ and $\varphi_{m,s}$ are calculated as follow respectively (Eqs. 39 and 40).

$$p(\omega_{\omega,s} \mid \theta) = c_1 \exp\left[-\frac{\left(\omega_{m,s}^{ur} - \omega_m^{ar}\right)^2}{2\varepsilon_m^2} \right] \tag{39}$$

$$p(\varphi_{m,s} \mid \theta) = c_2 \exp\left[-\frac{\left(\varphi_{m,s}{}_{m,s}^{ur} - \varphi_m^{ar}\right)^T \left(\varphi_{m,s}{}_{m,s}^{ur} - \varphi_m^{ar}\right)}{2{\delta_m}^2} \right] \tag{40}$$

where, $\varepsilon_m{}^2$ and $\delta_m{}^2$ are the variance of the m-th frequency and the diagonal element of covariance matrix C_m, respectively. The covariance matrix C_m of the m-th mode shape is simplified as $C_m=\delta_m{}^2 \mathrm{I}_{\mathrm{Nm}\times\mathrm{Nm}}$. The sample variances are used to approximate the variances of Gaussian distribution $\varepsilon_m{}^2$ and $\delta_m{}^2$ which can be calculated as follows (Eq. 41):

$$\varepsilon_m{}^2 = \frac{1}{N_s-1}\sum_{s=1}^{N_s}\left(\omega_{m,s}^{ur}-\bar{\omega}_m\right)^2, \qquad \delta_m{}^2 = \frac{1}{N_s-1}\sum_{s=1}^{N_s}\left\|\varphi_{m,s}{}_{m,s}^{ur}-\bar{\varphi}_m\right\|^2 \tag{41}$$

The prior distribution of model parameters θ is assumed to be uniform distribution, which means that its PDF has the form (Eq. 42):

$$p(\theta)=c_3 \tag{42}$$

where c_3 is a constant.

Substituting Eqs. 37 and 38 into Eq. 36, then combining Eqs. 36 and 40 yields the final form of $p(\theta|\mathrm{D})$ as shown in Eq. 43.

$$p(\theta \mid \mathrm{D}) = c\exp\left[-\sum_{s=1}^{N_s}\sum_{m=1}^{N_m}\left[\frac{\left(\omega_{m,s}^{ur}-\omega_m^{ar}\right)^2}{2\varepsilon_m^2}+\frac{\left(\varphi_{m,s}{}_{m,s}^{ur}-\varphi_m^{ar}\right)^T\left(\varphi_{m,s}{}_{m,s}^{ur}-\varphi_m^{ar}\right)}{2\delta_m^2}\right]\right] \tag{43}$$

The goal of Bayesian-based probabilistic analysis is to maximize the probability of $p(\theta|D)$ based on the known test data and then ascertain the most likely damaged elements. Based on the Bayesian analysis process, a multi-sample objective function is proposed to maximize the likelihood probability function $p(\theta|D)$, which can be converted into a minimization optimization problem written as Eq. 44. The aim of the multi-sample objective function is to make full use of the data sets but not use the average value only. The advantages of multi-sample objective function will be explored in the next section.

$$F=\arg min\left\{\sum_{s=1}^{N_s}\sum_{m=1}^{N_m}\left[\frac{\left(\omega_{m,s}^{ur}-\omega_m^{ar}\right)^2}{2\varepsilon_m^2}+\frac{\left(\varphi_{m,s}{}_{m,s}^{ur}-\varphi_m^{ar}\right)^T\left(\varphi_{m,s}{}_{m,s}^{ur}-\varphi_m^{ar}\right)}{2\delta_m^2}\right]\right\} \tag{44}$$

The values of θ, which causes the minimum value of objective function F are the obtained damage scenario.

Here, the global minima of objective function are considered as (0+tolerance limit). Tolerance limit is problem specific varying from 1×10^{-4} to 1×10^{-7} and will be mentioned during discussing each problem. The metaheuristic algorithm chosen is modified teaching-learning-based optimization (MTLBO) to obtain the correct damage location and damage severity utilizing the natural frequency and modeshapes based objective function. The analyses have been performed using an Intel Core i7-3632QM CPU 2.20 GHz processor with 8 GB of RAM on a 64-bit windows operating system.

3.3. Case study

In this section, two three-dimensional structures are presented for study:

a) 42-member three-dimensional flexural frame and
b) 120-member three-dimensional dome truss.

3.3.1. 42- Member space frame

A 42-bar space frame shown in Fig. 2 with multiple damage scenarios has been considered. The mechanical and geometric properties of the 3D frame are provided in the Table 1. Damage has been modelled as percentage reduction of the stiffness of the respective elements. Three failure scenarios have been considered. These failure scenarios are provided in the Table 2. Bayesian fusion results for all the damage cases are presented in Fig. 3. Table 3 reports the summary of suspected damaged locations for three discrete threshold values of 0.01, 0.001 and 0.0001. The results show that even for the threshold value as small as 0.0001, the fusion approach has detected damaged elements accurately. Now, the Bayesian fusion has also been applied to the

noisy data and results are reported in Fig. 3 along with summary of results in Table 3. Thus, for noisy environment the Bayesian fusion detected the damaged elements accurately for damage case DS1. In case of damage case DS2, the Bayesian fusion has detected one extra element than actual damage elements. In failure scenario number 3, where the number of damaged members is significantly higher than in the previous two scenarios, it is observed that only 2 additional members are considered. Therefore, in this method, it is evident that as the number of damaged members increases, the suspected members are identified with a very low error rate. So, the algorithm has detected a maximum of one extra damaged element than actual damaged elements. Thus, the proposed approach utilizing four damage indicators has substantially reduced the number of suspected damage elements in noise free and noisy environments.

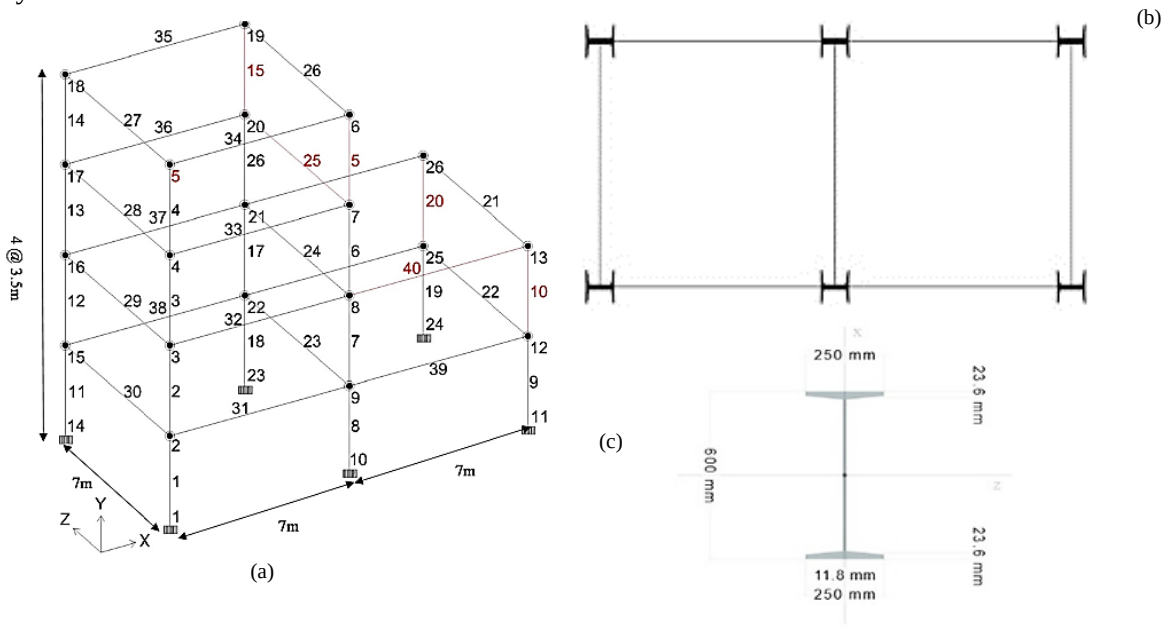


Fig. 2. 42-member space frame: (a) schematic diagram (red indicates damaged elements), (b) plan showing column orientation, (c) section adopted for beam and column.

Table 1. Geometric and mechanical properties of the members of a 42-member space frame.

	A(m^2)	**W(kg/m)**	**I_x(m^4)**	**I_y(m^4)**	**I_z(m^4)**	**υ**	**ρ(kg/m^3)**	**E(N/m)**
ISWB600	1.85×10^{-2}	145	5.30×10^{-5}	1.16×10^{-3}	1.21×10^{-3}	0.3	7837.84	2.1×10^{11}

Table 2. following two damage cases are chosen for 42-member space frame.

Damage scenario	**Member**	**5**	**10**	**15**	**20**	**25**					
DS1	Percentage of stiffness reduction	10%	15%	20%	25%	10%					
DS2	Member	5	10	15	20	25	40				
	Percentage of stiffness reduction	10%	15%	25%	20%	10%	15%				
DS3	Member	1	4	6	7	12	18	19	22	23	31
	Percentage of stiffness reduction	10%	15%	20%	25%	20%	15%	10%	5%	20%	25%

Table 3. Summary of damage detection results for 42-member space frame using various threshold values.

Damage	Free noise data		
	Threshold	**Actual damaged elements**	**Suspected damaged elements**
DS1	0.01	5,10,15,20,25	5,10,15,20
	0.001	5,10,15,20,25	5,10,15,20
	0.0001	5,10,15,20,25	5,10,15,20,25
DS2	0.01	5,10,15,20,25,40	5,10,15,20
	0.001	5,10,15,20,25,40	5,10,15,20,40
	0.0001	5,10,15,20,25,40	5,10,15,20,25,40
DS3	0.01	1,4,6,7,12,18,19,22,23,31	4,6,7,18,22,31
	0.001	1,4,6,7,12,18,19,22,23,31	1,4,6,7,18,19,22,31
	0.0001	1,4,6,7,12,18,19,22,23,31	1,4,4,6,7,12,18,19,22,23,31
Noise data			
DS1	0.01	5,10,15,20,25	5,10,15,20
	0.001	5,10,15,20,25	5,10,15,20
	0.0001	5,10,15,20,25	5,10,15,20,25
DS2	0.01	5,10,15,20,25,40	5,10,15,20,40
	0.001	5,10,15,20,25,40	5,10,15,20,25,40
	0.0001	5,10,15,20,25,40	5,8,10,15,20,25,40
DS3	0.01	1,4,6,7,12,18,19,22,23,31	4,6,7,11,18,20,22,23,31
	0.001	1,4,6,7,12,18,19,22,23,31	1,4,6,7,11,18,20,19,22,,23,31
	0.0001	1,4,6,7,12,18,19,22,23,31	1,4,6,7,11,12,18,19,22,23,31

In the shown figure, the identified faulty members are presented according to the failure scenarios described in three cases: the actual case, the Bayesian theory without noise, and the Bayesian theory with noise. As can be seen, very satisfactory results have been achieved. Even considering the increase in the number of affected members, identifying members suspected of damage is very close to reality.

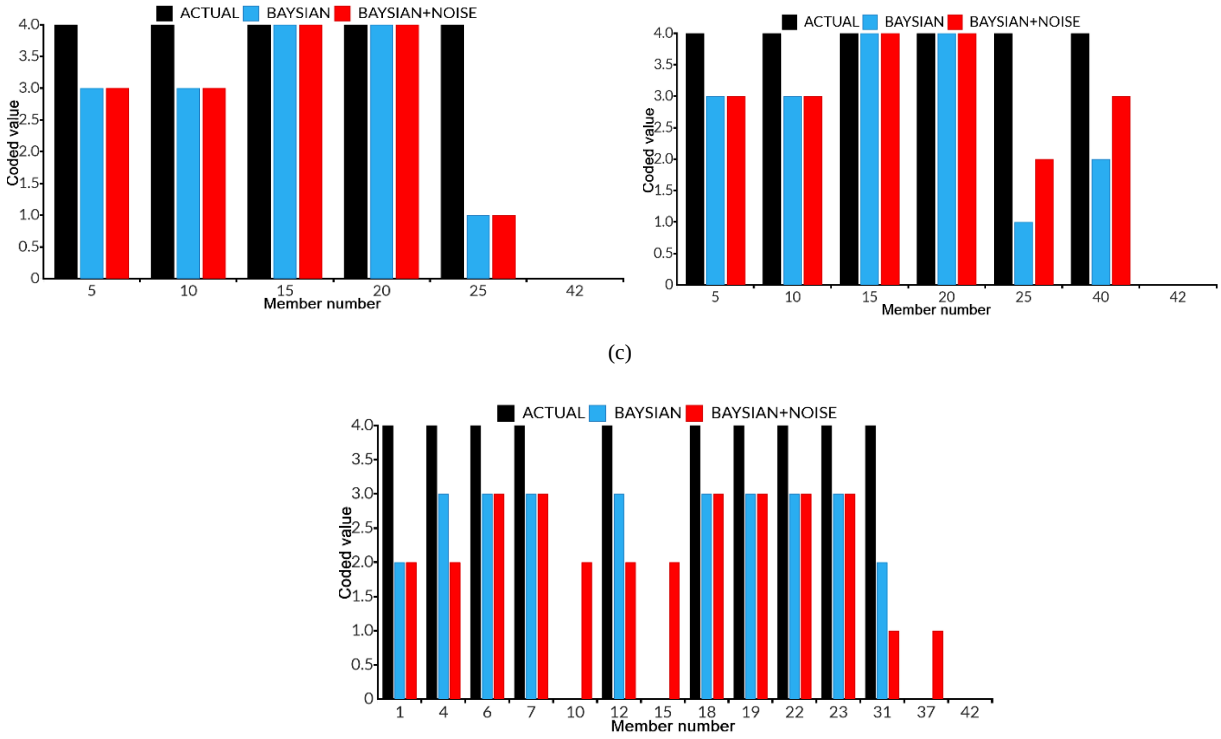
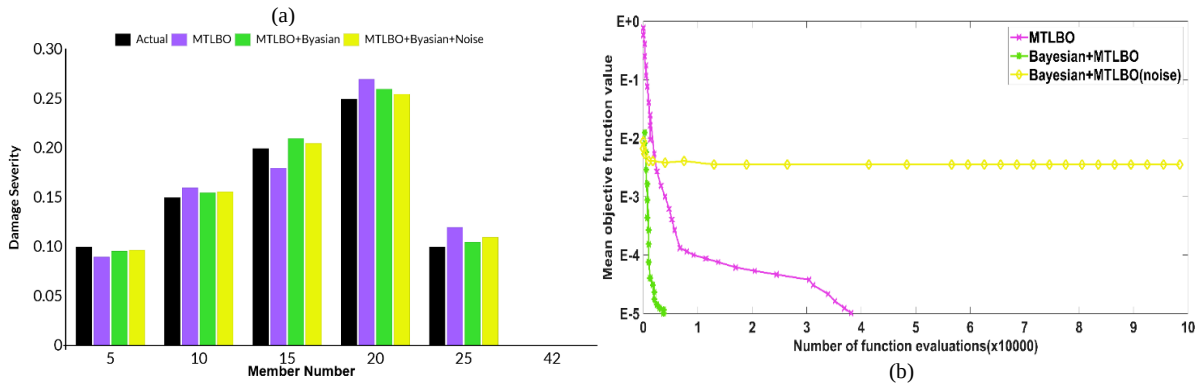


Fig. 3. Bayesian data fusion for detecting the damage locations using data from various damage indexes for 42-member space frame: (a) damage case DS1, (**b)** damage case DS2, (**c)** damage case DS3.

In the second stage of damage identification, the severity of the damage to the identified members from the previous step has been examined. Here, the impact of the introduced objective function and the MTLBO optimizer compared to the commonly used objective function in previous studies and the TLBO optimizer is discussed. The better and more precise quality of the proposed method is observable. Less susceptibility to noise, much

higher speed in the direction of convergence of the objective function, and results closer to reality indicate the better performance of the proposed method. An important point is the very low computational cost of the MTLBO algorithm compared to other optimization methods and its better results. The MTLBO algorithm has been employed to ascertain the accurate damage scenarios for damage cases DS1, DS2 and DS3 within both noise-free and noisy environments, enabling a comparative analysis between the Bayesian-MTLBO methodology and the conventional MTLBO approach. The parameters for swarm size, maximum iterations, and the minimum tolerance limit of the objective function have been established as 89, 300, and 1×10^{-5}, respectively. A total of twenty numerical iterations have been executed for each damage case. In light of the outcomes derived from Bayesian fusion, this investigation has exclusively considered 5 and 6 potential damage locations (optimization variables) for damage cases DS1, DS2 and DS3 respectively, in contrast to the 42 suspected damage locations (optimization variables) identified through the sole application of MTLBO (Rao et al., 2011). The Bayesian-MTLBO methodology has effectively evaluated damages in scenarios devoid of noise across all 20 numerical iterations, achieving an objective function value that falls below 1×10^{-5}. The damage prediction outcomes derived from the Bayesian-MTLBO strategy are illustrated in Figs 4a, 4c and 4e for damage scenarios DS1, DS2 and DS3 respectively. Consequently, the Bayesian-MTLBO has accurately identified both the locations and the severity of damages for the aforementioned cases. The mean convergence trajectories are depicted in Figs 4b, 4d and 4f for damage scenarios DS1, DS2 and DS3, respectively. The convergence trajectories indicate that the Bayesian-MTLBO methodology exhibits a superior convergence rate when juxtaposed with the traditional MTLBO approach. The computational duration has also been evaluated by averaging the time taken across 20 computations. The average time required to execute a single iteration for damage scenarios DS1, DS2 and DS3 is It has been shown table 4 that solely by the MTLBO methodology. The errors associated with damage predictions are significantly greater when employing only the MTLBO methodology. Specifically, for damage scenario DS3, the MTLBO has overestimated damage by 2% in member 9. Nevertheless, should the minimum tolerance threshold of the objective function be further diminished, it is plausible that the accuracy of damage predictions via the MTLBO could be enhanced. However, such an adjustment would concomitantly escalate the computational demands and time requisite. Conversely, the Bayesian-MTLBO has nearly flawlessly anticipated the damages across all elements within the established tolerance threshold of the objective function. Furthermore, the Bayesian-MTLBO algorithm has demonstrated commendable efficacy in environments characterized by noise. Therefore, one may deduce the superiority of the Bayesian-MTLBO methodology over the MTLBO in the context of detecting damages in frame structures, irrespective of the presence of noise. Additionally, the identification process is minimally affected by the presence of damage or its extent. This is attributed to the use of a probabilistic approach in both stages of damage identification.



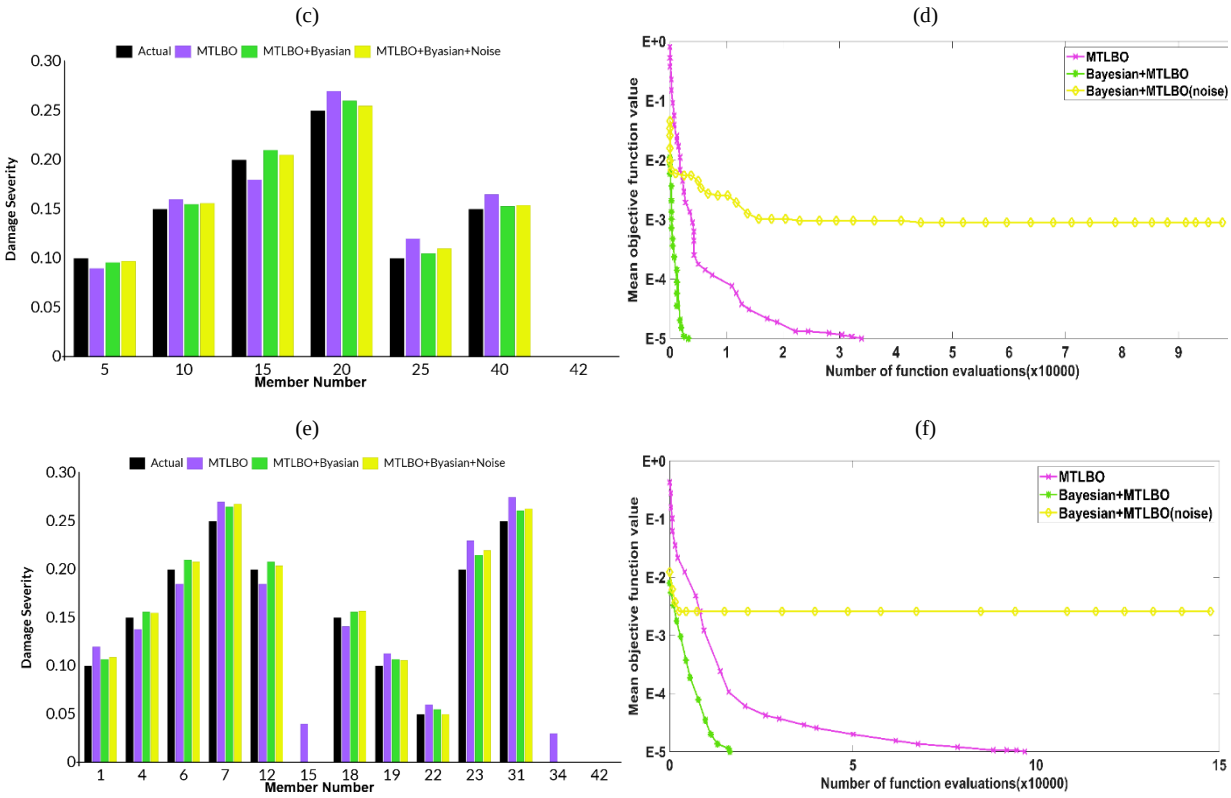


Fig. 4. Damage prediction of Bayesian-MTLBO approach for 42-member space frame: (**a)** damage prediction (DS1); (**b)** convergence curve (DS1); (**c)** damage prediction (DS2); (**d)** convergence curve (DS2); (**e)** damage prediction (DS3); (**f)** convergence curve (DS3).

Considering the multiple measurements in the proposed method for application in the proposed objective function, the process time has been slightly extended. This matter is presented in the table below. The effectiveness of adopting a two-step process in damage detection becomes significantly more pronounced considering the probabilistic nature of the objective function. This approach is particularly impactful for spatial frames, where its role is even more critical.

Table 4. Computational time (s) and number of function evaluations (NOF) for damage case DS1, DS2 and DS3 for 42-member space frame.

Algorithm	Computation Time (s)			NOFs		
	DS1	DS2	DS3	DS1	DS2	DS3
MTLBO	405	1380	2155	26580	50014	78256
Bayesian-MTLBO	38	84	123	1280	2355	4003

3.3.2. 120-bar 3D dome truss

A 120-bar dome truss with multiple damage scenarios has been considered for Bayesian data fusion (Fig. 5). The mechanical and geometric properties of the 3D frame are provided in the Table 5. Damage has been modelled as percentage reduction of the axial stiffness of the respective elements. Two failure scenarios have been considered. These failure scenarios are provided in the Table 6. The damage cases DS1 and DS2 have been used 17 to obtain the damaged locations and severity employing single-stage optimization. Figure 6 is constructed to present the Bayesian fusion results for all the damage cases. Summary of suspected damaged elements for all the cases are presented in Table 7 for three discrete threshold values of 0.01, 0.001 and 0.0001. Here, a maximum of four extra damaged elements have been detected even for the threshold value as small as 0.0001. Now, results of Bayesian fusion for noisy data are reported in Fig. 6a for damage case DS1 and Fig. 6b for damage case DS2 along with summary of results in Table 7. Thus, for noisy data the suspected damaged elements have been reduced in number to 6 in comparison with 8 for noise free data in case of damage case A5.

Also, in case of damage case DS2, the suspected damaged elements have been increased to 10 for noisy data compared to 6 for noise free data. So, the algorithm has detected a maximum of four extra damaged elements than actual damaged elements. Thus, the proposed approach has substantially reduced the number of suspected damage elements in noise free and noisy environments.

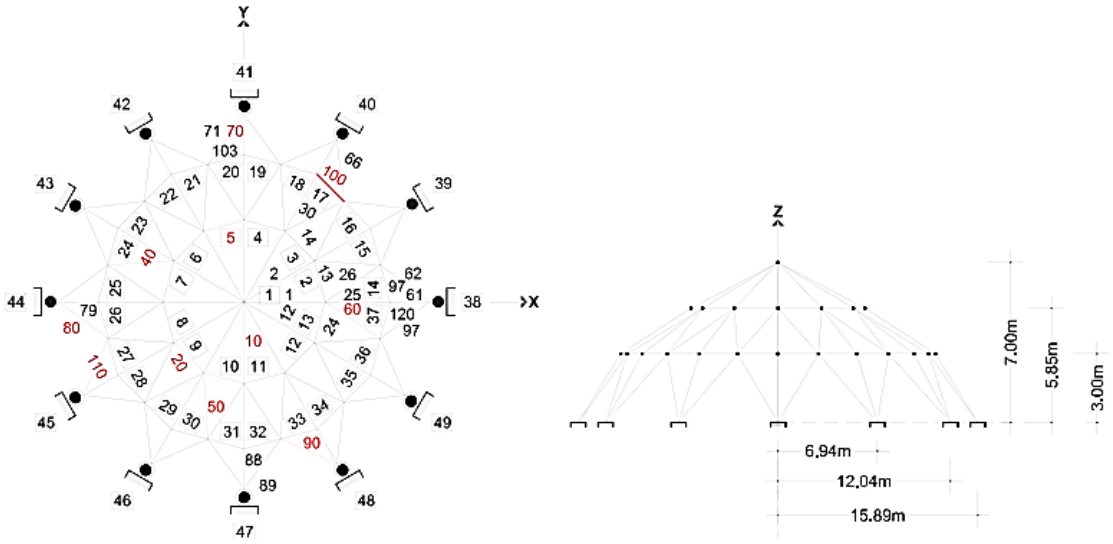


Fig. 5 Schematic diagram of 120 bar dome truss plan and elevation (red indicates damaged elements)

In the Table 5, the geometric and mechanical properties of the three-dimensional truss under study is presented.

Table 5. Geometric and mechanical properties of the members of a 120-bar 3D dome truss.

	A(m^2)	ρ(kg/m^3)	E(N/m)
Dome truss	0.0025	7971.81	2.1×10^{11}

Table 6. following two damage cases are chosen for 120-bar 3D dome truss.

Damage scenario							
DS1	Member	5	20	40	60	80	
	Percentage of stiffness reduction	10%	15%	25%	20%	10%	
DS2	Member	5	20	40	60	80	110
	Percentage of stiffness reduction	10%	15%	25%	20%	10%	15%

For the three-dimensional truss, two failure scenarios have been introduced. In the table below, the Bayesian theory was examined for two cases: without noise and with noise.

Table 7. Summary of damage detection results for 120-bar dome truss using various threshold values.

Damage	Free noise data		
	Threshold	**Actual damaged elements**	**Suspected damaged elements**
DS1	0.01	5,20,40,60,80	20,40,60,80 5,20,40,60,80 3,5,20,40,60,69,76,80
	0.001	5,20,40,60,80	
	0.0001	5,20,40,60,80	
DS2	0.01	5,20,40,60,80,110	20,40,60,80,110 5,20,40,60,80,110 5,20,40,60,80,110
	0.001	5,20,40,60,80,110	
	0.0001	5,20,40,60,80,110	
	Noise data		
DS1	0.01	5,20,40,60,80	20,40,60,80 5,20,40,60,80 3,5,20,40,60,80
	0.001	5,20,40,60,80	
	0.0001	5,20,40,60,80	
DS2	0.01	5,20,40,60,80,110	20,40,60,80,110 5,20,40,60,80,110 5,20,40,44,60,69,76,80,110,112
	0.001	5,20,40,60,80,110	
	0.0001	5,20,40,60,80,110	

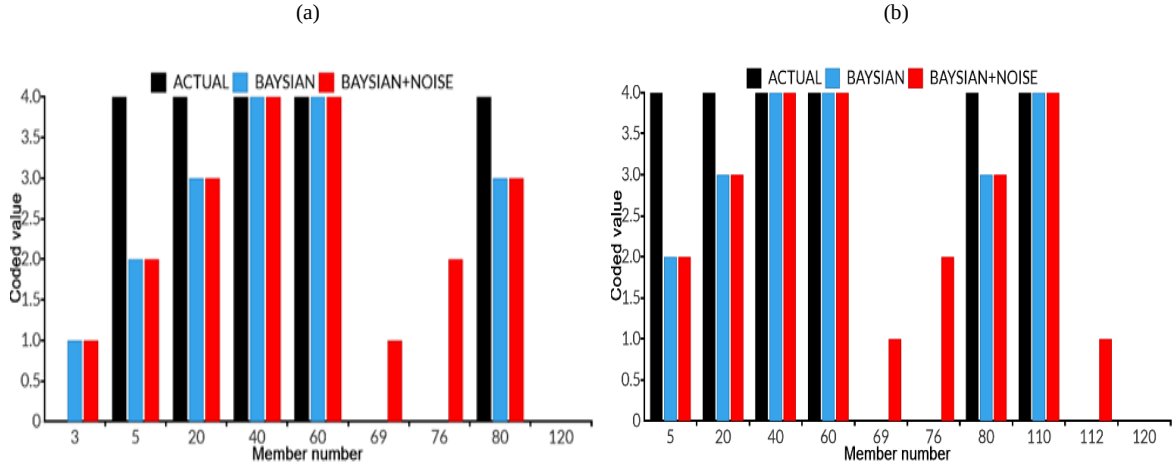


Fig. 6 Bayesian data fusion for detecting the damage locations using data from various damage indexes for 120-member space truss: (**a)** damage case DS1, **(b)** damage case DS2.

The MTLBO algorithm has been employed to ascertain the accurate damage scenarios pertaining to damage cases DS1 and DS2, thereby facilitating a comparative analysis between the contemporary Bayesian-MTLBO methodology. The parameters of swarm size, maximum iterations, and the minimum tolerance threshold for the objective function have been maintained in alignment with the specifications provided by Mishra et al., which are established at 110, 2500, and 1×10^{-5}, respectively. A total of twenty numerical simulations have been executed for each damage case. The Bayesian fusion methodology has effectively diminished the number of potential damage locations (optimization variables) to 8 and 6 for damage cases DS1 and DS2, respectively, while the single-stage MTLBO method utilized 120 potential damage locations (optimization variables). The Bayesian-MTLBO approach has yielded favorable outcomes in scenarios devoid of noise across all 20 numerical simulations, resulting in the objective function value falling below 1×10^{-5}. The damage detection scenarios facilitated by the Bayesian-MTLBO approach are illustrated in Fig. 7a and 7c for damage cases DS1 and DS2, respectively. The severity of the damage is determined from the simulations that exhibit the minimal objective function value. Consequently, both the damage locations and severity have been evaluated with a high degree of precision for both damage cases. The mean convergence curves are depicted in Fig. 7b and 7d for damage cases DS1 and DS2, respectively. The convergence curves distinctly illustrate the superiority of the Bayesian-MTLBO approach in comparison to the MTLBO approach concerning convergence velocity. The damage is meticulously identified utilizing the proposed Bayesian-MTLBO approach and remains within the accuracy threshold, attributable to the reduced number of control variables necessitated for optimization. Prior investigations utilizing solely the MTLBO method indicate that the lower bounds of damages are minimal in certain locations while significantly elevated in others, suggesting that the algorithm is deficient in its damage detection capabilities. What is noteworthy is that the proposed method has a lesser two-stage effect in determining the damage intensity in space trusses compared to frames. However, similar to frames, the number of convergence iterations and the ability to mitigate the impact of noise are quite significant.

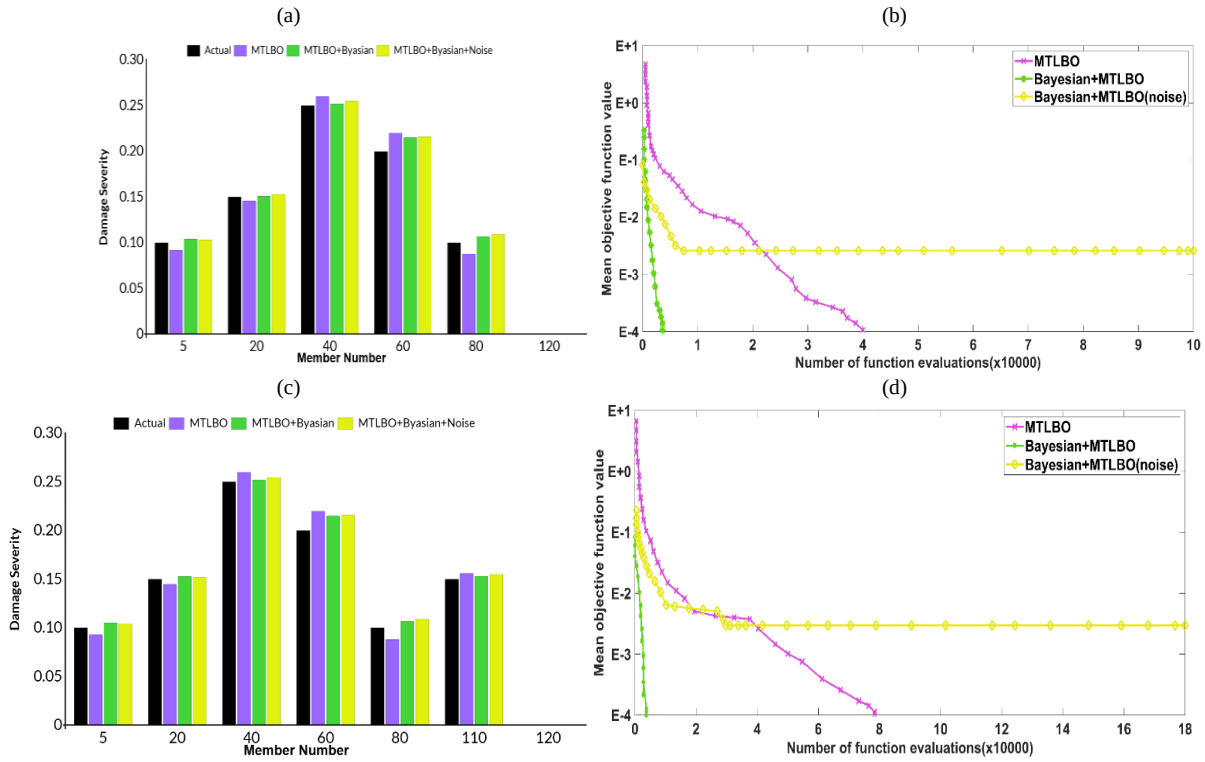


Fig. 7. Damage prediction of Bayesian-MTLBO approach for 120-member dome truss; (**a)** damage prediction (DS1); (**b)** convergence curve (DS1); (**c)** damage prediction (DS2); (**d)** convergence curve (DS2).

The table below presents the elapsed time for a 3D truss in both noise-free and noisy conditions. The computational time also has been calculated by considering the average time for 20 computations. It is observed that employing a two-step process in damage detection plays a highly effective role in reducing convergence time and minimizing optimization cycles. This becomes particularly significant when the utilized objective function is probabilistic, as it further enhances the process's efficiency. Thus, one can easily conclude in favor of Bayesian-MTLBO approach by observing the computational time, number of NOF reduction for both the damage cases and efficient prediction of damages in noisy environments (Table 8).

Table 8. Computational time (s) and number of function evaluations (NOF) for damage case DS1 and DS2 for 120-bar dome truss.

Algorithm	Computation Time (s)		NOFs	
	DS1	DS2	DS1	DS2
MTLBO	7256	9825	123124	134123
Bayesian-MTLBO	560	621	6925	6825

4. Conclusions

This study presents a two-stage inverse damage detection method that integrates Bayesian fusion with metaheuristic optimization based on vibration parameters. Two structural models a 42-member space frame and a 120-member dome truss are used to evaluate the proposed method against traditional single-stage optimization-based approaches. The MTLBO algorithm is adopted as the primary optimization tool. In the first stage, Bayesian fusion is employed to identify potentially damaged elements using a predefined threshold, combining information from four damage indices derived from modal strain energy (MSE), modal flexibility, frequency response functions (FRF), and modal residual force. The results demonstrated that incorporating Bayesian fusion significantly reduced the number of falsely identified damaged elements. Even at a very low threshold of 0.0001, the number of additional suspected elements beyond the actual damaged ones was limited to 0–4. In the second stage, a probabilistic objective function, formulated

based on Bayesian probability theory, was employed to accurately estimate the damage severity. The Modified Teaching–Learning-Based Optimization (MTLBO) algorithm is employed to minimize the probabilistic objective function derived from Bayesian probability theory. In contrast to conventional single-stage optimization methods where all structural elements are treated as potential damage sites the proposed two-stage approach demonstrates superior accuracy in damage identification, even when the tolerance limit of the objective function is relatively high. This improvement is confirmed through the space frame example. Furthermore, the algorithm's robustness was evaluated under noisy data conditions. The Bayesian fusion stage effectively reduced the number of suspected damaged elements despite the noise, thereby expediting the second-stage damage severity assessment. Consequently, the overall performance of the proposed methodology remains stable and reliable even in the presence of measurement noise. In this two-stage framework, the application of Bayesian theory in the first stage for identifying potentially damaged members, combined with the use of an enhanced optimization algorithm in the second stage, has improved the overall convergence rate of the results. However, the probabilistic formulation of the objective function introduces additional computational effort, making each iteration relatively time-consuming. This increased computational demand arises from the need to process real-time measurements and continuously update statistical parameters throughout the iterative procedure. The proposed two-stage method demonstrates higher sensitivity in 3D frames than in trusses and provides rapid convergence and high accuracy in damage detection. It is scalable for various structural sizes and adaptable to the number of available damage indicators. The approach performs well even with noisy data, making it suitable for large-scale and real-world structures. By combining Bayesian fusion and an enhanced learning-based optimization algorithm, the method effectively reduces noise sensitivity, improves convergence speed, and minimizes errors. Due to its low computational cost and robust probabilistic formulation, it outperforms traditional single-stage techniques. Future work could explore its performance under different noise levels and extend its use to joint damage detection.

Acknowledgements

This research was not funded by any organization or institution.

References

Alkayem, N.F. & Cao, M., 2018. Damage identification in three-dimensional structures using single-objective evolutionary algorithms and finite element model updating: evaluation and comparison. *Engineering Optimization*, 50(10), pp.1695-1714.

Bagherahmadi, S.A. & Seyedpoor, S.M., 2018. Structural damage detection using a damage probability index based on frequency response function and strain energy concept. *Structural Engineering and Mechanics*, 67(4), pp.327-336.

Barman, S.K., Jebieshia, T.R., Tiwari, P., Maiti, D.K. & Maity, D., 2019. Two-stage inverse method to detect delamination in composite beam using vibration responses. *AIAA Journal*, 57(3), 1312-1322.

Barman, S.K., Mishra, M., Maiti, D.K. & Maity, D., 2021. Vibration-based damage detection of structures employing Bayesian data fusion coupled with TLBO optimization algorithm. *Structural and Multidisciplinary Optimization*, 64(4), 2243-2266.

Cedeño-Rodríguez, M.D., Yanez, S.J., Saavedra-Flores, E.I., Guzmán, C.F. & Pina, J.C., 2025. Vibration-Based Damage Prediction in Composite Concrete–Steel Structures Using Finite Elements. *Buildings*, 15(2), p.200.

Cruz, P.J. & Salgado, R., 2009. Performance of vibration-based damage detection methods in bridges. *Computer-Aided Civil and Infrastructure Engineering*, 24(1), 62-79.

Das, S., Saha, P. & Patro, S.K., 2016. Vibration-based damage detection techniques used for health monitoring of structures: a review. *Journal of Civil Structural Health Monitoring*, 6(3), pp.477-507.

Das, T. & Guchhait, S., 2024. A 2D-CNN-based two-stage structural damage localization and quantification technique using time domain vibration data. *International Journal of Structural Stability and Dynamics*, 24(20), p.2450232.

Dinh-Cong, D., Vo-Duy, T., Ho-Huu, V. & Nguyen-Thoi, T., 2019. Damage assessment in plate-like structures using a two-stage method based on modal strain energy change and Jaya algorithm. *Inverse Problems in Science and Engineering*, 27(2), pp.166-189.

Dinh-Cong, D., Vo-Duy, T., Ho-Huu, V. & Nguyen-Thoi, T., 2019. Damage assessment in plate-like structures using a two-stage method based on modal strain energy change and Jaya algorithm. *Inverse Problems in Science and Engineering*, 27(2), pp.166-189.

Fan, W. & Qiao, P., 2011. Vibration-based damage identification methods: a review and comparative study. *Structural Health Monitoring*, 10(1), 83-111.

Gerist, S. & Maheri, M.R., 2016. Multi-stage approach for structural damage detection problem using basis pursuit and particle swarm optimization. *Journal of Sound and Vibration*, 384, 210-226.

Ghasemi, M.R., Nobahari, M. & Shabakhty, N., 2018. Enhanced optimization-based structural damage detection method using modal strain energy and modal frequencies. *Engineering with Computers*, 34(3), pp.637-647.

Ghiasi, R., Fathnejat, H. & Torkzadeh, P., 2019. A three-stage damage detection method for large-scale space structures using forward substructuring approach and enhanced bat optimization algorithm. *Engineering with Computers*, 35(3), pp.857-874.

Hızal, Ç. & Aktas, E., 2021. Structural Health Monitoring-Integrated Reliability Assessment of Engineering Structures. In *Reliability-Based Analysis and Design of Structures and Infrastructure* (pp. 117-128). CRC Press.

Humar, J., Bagchi, A. & Xu, H., 2006. Performance of vibration-based techniques for the identification of structural damage. *Structural Health Monitoring*, 5(3), pp.215-241.

Kaveh, A. & Zolghadr, A., 2017. Cyclical parthenogenesis algorithm for guided modal strain energy based structural damage detection. *Applied Soft Computing*, 57, 250-264.

Kim, J.T. & Stubbs, N., 2002. Improved damage identification method based on modal information. *Journal of Sound and Vibration*, 252(2), 223-238.

Li, W., Fan, Y. & Xu, Q., 2020. Teaching-learning-based optimization enhanced with multiobjective sorting based and cooperative learning. *IEEE Access*, 8, 65923-65937.

Machado, M.R., Adhikari, S. & Dos Santos, J.M.C., 2017. A spectral approach for damage quantification in stochastic dynamic systems. *Mechanical Systems and Signal Processing*, 88, 253-273.

Mishra, M., Barman, S.K., Maity, D. & Maiti, D.K., 2020. Performance studies of 10 metaheuristic techniques in determination of damages for large-scale spatial trusses from changes in vibration responses. *Journal of Computing in Civil Engineering*, 34(2), 04019052.

Montalvao, D., Maia, N.M.M. & Ribeiro, A.M.R., 2006. A review of vibration-based structural health monitoring with special emphasis on composite materials. *Shock and Vibration Digest*, 38(4), pp.295-324.

Montazer, M. & Seyedpoor, S.M., 2014. A new flexibility based damage index for damage detection of truss structures. *Shock and Vibration*, *2014*(1), p.460692.

Niu, P., Ma, Y. & Yan, S., 2019. A modified teaching–learning-based optimization algorithm for numerical function optimization. *International Journal of Machine Learning and Cybernetics*, 10(6), 1357-1371.

Pandey, A.K. & Biswas, M., 1994. Damage detection in structures using changes in flexibility. *Journal of Sound and Vibration*, 169(1), pp.3-17.

Radzieński, M., Krawczuk, M. & Palacz, M., 2011. Improvement of damage detection methods based on experimental modal parameters. *Mechanical Systems and Signal Processing*, 25(6), 2169-2190.

Rao, R.V., Savsani, V.J. & Vakharia, D.P., 2011. Teaching–learning-based optimization: a novel method for constrained mechanical design optimization problems. *Computer-Aided Design*, 43(3), pp.303-315.

Ruiz, D.V., de Braganca, C.S.C., Poncetti, B.L., Bittencourt, T.N. & Futai, M.M., 2024, January. Vibration-based structural damage detection strategy using FRFs and machine learning classifiers. In *Structures* (Vol. 59, p. 105753). Elsevier.

Ruiz, D.V., de Bragança, C.S.C., Poncetti, B.L., Bittencourt, T.N. & Futai, M.M., 2025. Structural damage detection for a small population of nominally equal beams using PSO-optimized Convolutional Neural Networks. *Mechanical Systems and Signal Processing*, *225*, 112276.

Salawu, O.S., 1997. Detection of structural damage through changes in frequency: a review. *Engineering Structures*, 19(9), 718-723.

Shekhar, S., Freddi, F., Ghosh, J. & Lad, D., 2023. Influence of corrosion on failure modes and lifetime seismic vulnerability assessment of low-ductility RC frames. *Earthquake Engineering & Structural Dynamics*, 52(15), 5162-5184.

Shi, Z.Y., Law, S.S. & Zhang, L.M., 2002. Improved damage quantification from elemental modal strain energy

change. *Journal of Engineering Mechanics*, 128(5), 521-529.

Shih, H.W., Thambiratnam, D.P. & Chan, T.H.T., 2009. Vibration based structural damage detection in flexural members using multi-criteria approach. *Journal of Sound and Vibration*, 323(3-5), 645-661.

Simoen, E., De Roeck, G. & Lombaert, G., 2015. Dealing with uncertainty in model updating for damage assessment: A review. *Mechanical Systems and Signal Processing*, 56, 123-149.

Tibaduiza Burgos, D.A., Gomez Vargas, R.C., Pedraza, C., Agis, D. & Pozo, F., 2020. Damage identification in structural health monitoring: A brief review from its implementation to the use of data-driven applications. *Sensors*, 20(3), 733.

Vamvoudakis-Stefanou, K.J., Sakellariou, J.S. & Fassois, S.D., 2018. Vibration-based damage detection for a population of nominally identical structures: Unsupervised Multiple Model (MM) statistical time series type methods. *Mechanical Systems and Signal Processing*, 111, 149-171.

Yan, A.M., Kerschen, G., De Boe, P. & Golinval, J.C., 2005. Structural damage diagnosis under varying environmental conditions—Part I: A linear analysis. *Mechanical Systems and Signal Processing*, 19(4), 847-864.

Zhang, Y. & Yang, W., 2013. Bayesian strain modal analysis under ambient vibration and damage identification using distributed fiber Bragg grating sensors. *Sensors and Actuators A: Physical*, 201, 434-449.